We are IntechOpen, the world's leading publisher of Open Access books Built by scientists, for scientists

4,800
Open access books available

122,000
International authors and editors

135M
Downloads

Our authors are among the

154
Countries delivered to

TOP 1%
most cited scientists

12.2%
Contributors from top 500 universities

WEB OF SCIENCE™

Selection of our books indexed in the Book Citation Index in Web of Science™ Core Collection (BKCI)

Interested in publishing with us?
Contact book.department@intechopen.com

Numbers displayed above are based on latest data collected.
For more information visit www.intechopen.com

31

Transport of Ultradispersed Catalytic Particles Through Bitumen at Upgrading Temperatures

Herbert Loria and Pedro Pereira-Almao
Chemical & Petroleum Engineering Department, University of Calgary
Canada

1. Introduction

Mass transfer and deposition of fine particles in cylindrical channels has received considerable attention for a long time due to its practical significance and direct application in industry. For example, this knowledge is helpful in aerosol classification and its deposition under electrical fields, formation of deposits in heat exchangers and pipelines, hydrodynamic field chromatography, thrombus formation in organs and, many other areas (Adamczyk and Van De Ven, 1981). Recently, this phenomenon has gained particular importance on the dispersion of ultradispersed catalysts for heavy crude oil and bitumen hydroprocessing due to its practical significance and direct application (Pereira-Almao et al., 2007; Galarraga and Pereira-Almao, 2010; Loria et al., 2011).

Ultradispersed catalysts have been studied for heavy oil and bitumen hydroprocessing as an alternative for typical supported catalysts. An advantage when comparing ultradispersed catalysts to supported ones, in the case of heavy oil and bitumen hydroprocessing, is that the former could be easily incorporated into the reaction media to flow together with the feedstock to be treated, in this manner residence times can be longer than those conventionally used for hydroprocessing (Pereira-Almao et al., 2005; Pereira-Almao, 2007).

Recent publications (Loria et al., 2009b, 2009c, 2010) have demonstrated the feasibility of the transport of ultradispersed particles based on their motion through diverse viscous media enclosed in horizontal cylindrical channels. Time-dependent, two and three-dimensional convective-dispersive models, which simulated the transient deposition and suspension of ultradispersed particles immersed in viscous media inside a horizontal cylinder, were developed, solved and experimentally validated. In addition, a study on the effect of the fluid medium properties over the dispersion coefficient was performed. The dispersion coefficient is a proportionality constant that serves to quantify the particle concentration due to convection and dispersion and should be expressed as a function of the properties of the fluid medium (Loria et al., 2010).

The solution of the previously mentioned models provides a particle concentration profile along the horizontal channel, as well as information regarding the critical particle size that allows particles to remain suspended in the fluid medium enclosed in this geometry. This knowledge can be applied in the previously referred ultradispersed catalysis of heavy crude oils and bitumen. In these systems, it is important to ensure that catalytic particles remain suspended in the fluid medium in order to make use of their catalytic activity and also, to

obtain the conditions for which these particles will sediment in order to recover and reuse them in recirculation systems.

The present study intends to show the application of the convective-dispersive models in cases that involve the storage and transport of catalytic particles immersed in bitumen at upgrading temperatures (340 -380° C) inside cylindrical geometries.

The main objective of this paper is to employ the previously developed models as tools for interpretation of cases of interest for the heavy oil and bitumen industry. The modelling parameters of these systems can be based on those employed in the validation experiments for the convective-dispersive models (Loria et al., 2009b, 2009c, 2010), since physical properties from particles and fluids used in the experiments were deliberately chosen to be similar as those that catalytic particles and bitumen would have at upgrading temperatures.

The first part of this paper deals with a large scale application of the two-dimensional convective-dispersive model (Loria et al., 2009b, 2009c). Since this model predicts the particle concentration profile enclosed in a circumference, it can be applied to the cross-sectional part of a spherical storing tank. In this section, the concentration profile of molybdenum trioxide (MoO_3) catalytic particles immersed in bitumen enclosed in a 4 m diameter spherical tank is studied.

The second section of this paper is related to the three-dimensional convective-dispersive model (Loria et al., 2010). This model simulates the transient deposition and suspension of particles immersed in a fluid travelling through a horizontal cylindrical channel and provides the particle concentration profile along the channel. In this case, simulations involving a pipe of 100 m length and 101.6 cm diameter transporting MoO_3 catalytic particles immersed in bitumen were carried out.

The simulations took into account different particle diameters, ranging from 1 to 1500 nm and different temperatures, ranging from 340 to 380° C. The bitumen's physical properties (density and viscosity) vary with respect to the different studied temperatures and are essential inputs of the convective-dispersive model. In order to obtain these properties; a previously developed thermodynamic model for their calculation (Loria et al., 2009a) was employed.

2. Two-dimensional transport of particles through viscous fluid media

2.1 Two-dimensional convective-dispersive model to predict the concentration profile of particles immersed in viscous media

When a particle settles down in a liquid medium, it accelerates until the forces that cause the sedimentation equilibrate with the resistance or drag forces offered by the medium. Once this equilibrium is achieved, the particle has a constant sedimentation velocity called terminal sedimentation velocity (v_{pT}) which can be represented by (Ramalho, 1983):

$$v_{pT} = \frac{g\left(\rho_p - \rho_L\right)d_p^2}{18\mu_L}, \tag{1}$$

where g is the acceleration due to gravity, ρ_p is the density of the particle, ρ_L is the density of the liquid, d_p is the diameter of the particle and μ_L is the viscosity of liquid medium. Equation 1 is also known as the Stokes' law for the sedimentation of discrete particles.

A continuity equation for the particle concentration in a fluid medium can be obtained by carrying out a mass balance on a differential element of volume. Considering that particle

concentration (C_P) varies with time (t), that the effective dispersion coefficient (D_E) is constant, that the particle concentration inside a cylindrical channel is modelled as a function of the position of the particles in the cross-section of the cylinder and the time, $C_P = C_P\ (r,\ \theta,\ t)$, that the angular velocity of the particle (v_θ) is small compared to the radial velocity (v_r) and that this radial velocity can be obtained by projecting the vertical terminal velocity of the particle into the radial direction ($v_r = v_{PT}\cos\theta$); then the continuity equation in cylindrical coordinates can be written as (Bird et al., 2007):

$$\frac{\partial C_P}{\partial t} + v_{pT}\cos\theta\frac{\partial C_P}{\partial r} = D_E\left[\frac{1}{r}\frac{\partial}{\partial r}\left(r\frac{\partial C_P}{\partial r}\right) + \frac{1}{r^2}\frac{\partial^2 C_P}{\partial \theta^2}\right]. \tag{2}$$

D_E is called the effective dispersion coefficient because the transport of the particles from high concentrated areas to low concentrated ones is, in this case, due to their mixing with the liquid bulk (Franco, 2008) and it is called effective because includes the motion effects caused by the particles and the gravity force in all directions. It distinguishes from the diffusivity coefficient in the sense that diffusivity is determined by the molecular properties of the particles and the fluid in which they are immersed, whereas the dispersion coefficient is determined by the particle properties and fluid conditions. Generally, in atmospheric transport, dispersive flux dominates the diffusive flux.

In the beginning of the process ($t = 0$) all particles are well dispersed inside the cross section of the cylindrical channel. This means that particle concentration is uniform everywhere inside the cross-section of the cylindrical channel. This concentration is the initial concentration of the particles (C_{P0}).

$$\text{At } t = 0,\ C_P(r, \theta, 0) = C_{P0},\ 0 < r < R, 0 < \theta < 2\pi. \tag{3}$$

In the vertical axis there are symmetry boundary conditions that can be represented as:

$$\text{At } \theta = 0,\ \frac{\partial C_P}{\partial \theta} = 0\ ,\ 0 < r < R. \tag{4}$$

$$\text{At } \theta = \pi,\ \frac{\partial C_P}{\partial \theta} = 0\ ,\ 0 < r < R. \tag{5}$$

In the centre of the cylindrical channel the particle concentration does not vary with respect to the radius around all the angles:

$$\text{At } r = 0,\ \frac{\partial C_P}{\partial r} = 0\ ,\ 0 < \theta < 2\pi. \tag{6}$$

The walls of the channel represent a physical boundary where there is no mass exchange between the interior and exterior of the cylinder. This is an insulation boundary that will prevent any particle from leaving the channel, gathering all settled particles at the bottom. The insulation boundary means that there is no convective or dispersive flux across that boundary. This can be represented by:

$$\text{At } r = R,\ -D_E\frac{\partial C_P}{\partial r} + \left(v_{pT}\cos\theta\right)C_P = 0\ ,\ 0 < \theta < 2\pi. \tag{7}$$

The convective-dispersive model is a linear second order parabolic partial differential equation; this equation can be solved by a large variety of numerical methods: finite differences, finite element, finite volume, characteristics methods, discontinuous Garlekin methods, etc. A numerical solution based in the finite element method was used to solve this equation. This solution presented good convergence and stability properties due to the regular grid structure and its flexibility with respect to the adaptation to the geometry domain. Computational fluid dynamics software was used in order to apply the method.

2.2 Effect of the fluid medium properties on the dispersion coefficient

Two of the parameters which are necessary input data for the numerical solution of the convective-dispersive model are v_{pT} and D_E. They can be obtained from experimental physical parameters. The calculation of v_{pT} can be performed directly from equation 1. However; the effective dispersion coefficient of the particles, D_E, cannot be obtained directly from any formula, the best way to obtain this value is to perform an adjustment of this parameter using concentration values from experimental data.

In a previous work (Loria et al., 2009c), a study to observe the variation of the dispersion coefficient with respect to the changes of the properties of the fluid medium was performed. For this study the experimental data collected from Fe_2O_3 nanoparticles immersed in different mixtures of water and glycerol was used.

Figure 1 shows the behaviour of the dispersion coefficient with respect to an increase of density and viscosity of the fluid medium. It can be observed that as the fluid medium becomes denser and more viscous the dispersion coefficient decreases. The particles gradually decrease their capability to move as the fluid medium becomes denser and more viscous; thus, the particles lose their ability to go from high concentrated areas to low concentrated ones, causing a decrease of the dispersion coefficient. These experimentally obtained dispersion coefficients showed a tendency to increase when the conditions were more favourable for sedimentation, that is, low density and viscosity

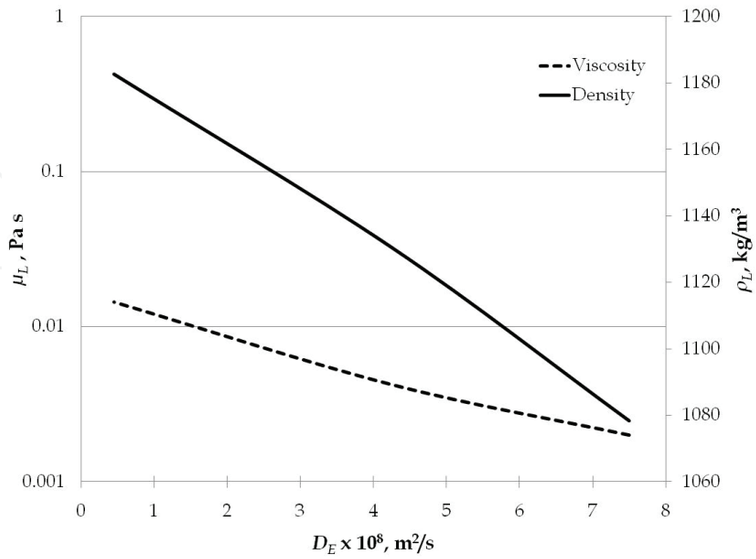

Fig. 1. Dispersion coefficient (D_E) as a function of the viscosity (μ_L) and density (ρ_L) of the fluid medium in the cross-section of a horizontal cylinder

Literature data related to cross-sectional dispersion coefficients in horizontal channels is scarce. The dispersion coefficient obtained in this research could be compared to the diffusion coefficients obtained by (d'Orlyé et al., 2008). They studied diffusion coefficients of maghemite particles (γ-Fe_2O_3) dispersed in an aqueous solution of nitric acid. They performed diffusion coefficient measurements for nanometric particles (< 10 nm) based on the results of dynamic light scattering experiments in the cross-section of horizontal capillary tube. They obtained diffusion coefficients in the order of 10^{-11} m^2/s, which varied three orders of magnitude from the D_E values obtained in this work. This difference is probably due to the use of particles smaller than 10 nm, the employment of capillary tubes of 50 μm of diameter and the use of dynamic light scattering results for the calculation of particle concentrations since dynamic light scattering is a technique primarily designed for particle size measurement.

Dispersion coefficients with similar orders of magnitude as the ones obtained in a previous work (Loria et al., 2009c) carried out with submicron particles (10^{-8} -10^{-9} m^2/s) were found by (Robbins, 1989; Massabò et al., 2007). However, these results are not comparable with this work since they performed their calculations in a packed column based on concentration measurements that were generated by the computational simulation of a continuous tracer injection experiment in a vertical cylindrical geometry.

2.3 Ultradispersed catalytic particles immersed in bitumen at upgrading temperatures stored inside a spherical tank

In this section, the two-dimensional convective-dispersive model is applied to a large scale case which involves the storage of MoO_3 catalytic particles immersed in Athabasca bitumen, at upgrading conditions (340-380 °C), inside a 4 m diameter spherical tank.

The objectives of this study are: to find the critical particle diameter for its suspension, and to calculate the deposited mass of the catalytic particles at the bottom of the tank once the steady state has been reached.

The density (ρ_L) and viscosity (μ_L) of the Athabasca bitumen at five different temperatures ranging from 340 to 380 °C were employed in the following simulations. These physical properties were calculated with thermodynamic models for the prediction of density and viscosity of heavy crude oil and bitumen, details of these models were presented by (Loria et al., 2009a). Table 1 shows the densities and viscosities of Athabasca bitumen in the range 340 to 380 °C, these values were obtained with the previously mentioned thermodynamic models.

T, °C	ρ_L, kg/m^3	μ_L, cP
340	884.7	2.71
350	877.2	2.42
360	869.4	2.38
370	856.4	2.27
380	843.7	2.17

Table 1. Densities and viscosities of the Athabasca bitumen in the range 340 to 380 °C

MoO_3 (ρ_p = 4700 kg/m^3 (Perry, 1997)) particle diameters which were used for the simulations ranged from 1 to 1500 nm. In total fourteen different particle diameters were studied: 1, 10, 50, 100, 150, 200, 250, 300, 400, 500, 750, 1000, 1250 and 1500 nm.

The initial MoO_3 particle concentration (C_{P0}) applied to all the simulations was 1.2526 mol/m^3. A common concentration unit employed in ultradispersed catalysis for hydroprocessing is ppm (parts per million or g/m^3). In this case, 1.2526 mol/m^3 are equivalent to 180.3 ppm. This particle concentration is within the same magnitude order as those that have been proposed for ultradispersed catalysis for hydroprocessing (Pereira-Almao, 2007).

The calculation of the dispersion coefficient that was used for these simulations was based on the results that were obtained when the two-dimensional convective-dispersive model was validated with Fe_2O_3 particles immersed in mixtures of water and glycerol (Loria et al., 2009c). These data were used since particle properties and concentrations in addition to the fluid medium characteristics used in those experiments are similar to those employed in the simulations carried out in this section.

The dispersion coefficient calculation was carried out in the following way: polynomial interpolations were applied to the data from Figure 1 (μ_L and ρ_L vs. D_E); then, for each temperature a pair of D_E values were obtained (one based on μ_L and the other in ρ_L) and their average was recorded; finally, the 5 different D_E average values (corresponding to each one of the studied temperatures and ranging from 4.9 - 5.6 × 10^{-8} m^2/s) were averaged and the final D_E value was obtained. The D_E value obtained from these calculations resulted to be 5.33 × 10^{-8} m^2/s.

A total of 70 different simulations were carried out in this section (based on the 14 different particle diameters and 5 different temperatures). Computational fluid dynamics was used to perform the simulations; each simulation was carried out up to a time of 1 × 10^8 s (27778 h), a time long enough to reach the steady state in each one of them. 2508 grid points were employed for the solution of each simulation and their computing time was around 60 s

A point of interest in this study is the critical particle diameter for deposition; that is, the particle diameter from which particles with higher sizes will be deposited and particles with lower sizes will remain suspended. In order to measure this new parameter, the following analysis was conducted.

The normalized maximum particle concentration, which is the concentration that is found at the bottom of the circumference after the simulation time (steady state) divided by the initial concentration, was calculated for each simulation. When the normalized maximum concentration tends to the initial one (normalized concentration = 1), it means that there is no particle deposition at the bottom of the circumference.

This normalized maximum particle concentration was plotted against the particle diameter in order to observe at which particle diameter the maximum particle concentration becomes significant. Figure 2 represents the behaviour of the normalized maximum particle concentration at different particle diameters and temperatures.

As temperature increases for a specific particle diameter, the normalized maximum concentration increases. Also, as the particle diameter increases, the normalized maximum concentration increases for a constant temperature. It can also be observed that a change in particle diameter have a more pronounced effect over the normalized maximum concentration than a change in temperature.

In the particle diameter axis, there is a zone for values lower than 150 nm where the normalized maximum concentration is equal to the initial one independently of the studied temperature. This means that MoO_3 particles smaller than 150 nm will remain suspended in the Athabasca bitumen after a long period of time (1 × 10^8 s) in the range of temperatures from 340 to 380 °C.

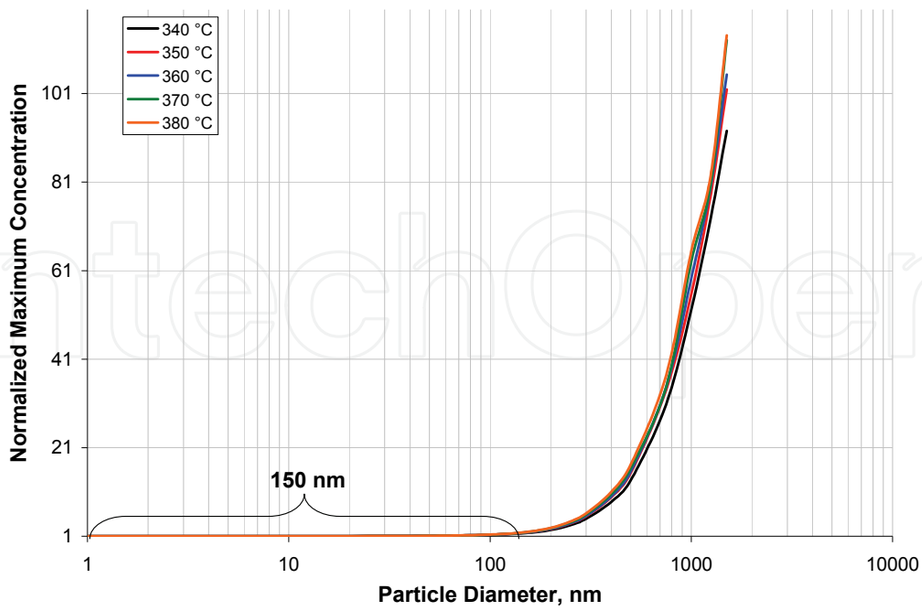

Fig. 2. Effect of the particle diameter and temperature on the deposition of MoO_3 particles immersed in Athabasca bitumen enclosed in a spherical tank of 4 m diameter

In order to calculate the deposited mass of the catalytic particles at the bottom of the spherical tank once the steady state has been reached, the following procedure was employed.
Assuming that the deposited particles filled a small gap of height H at the bottom of the spherical tank of radius R, its volume (V_P) can be calculated by:

$$V_P = \frac{1}{3}\pi H^2 (3R - H) \tag{8}$$

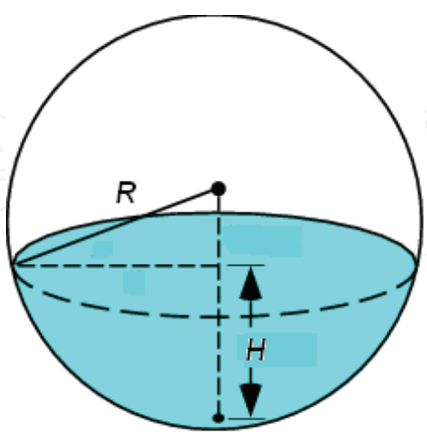

Fig. 3. Gap of height H at the bottom of a spherical tank of radius R

Assuming that the height of this small gap is approximately H = 6.5 cm (based on the simulation results), the volume of the gap (V_P) for a sphere of 2 m of radius is 1.73 $\times 10^{-3}$ m^3.

Since particle concentration in this part of the tank after a long period of time is already known from the simulation results, i.e. the maximum particle concentration ($C_{P\max}$), then the deposited mass (M_P) is:

$$M_P = C_{P\max} V_P \tag{9}$$

On the other hand, the total mass of the immersed particles inside the tank (M_{PT}) is:

$$M_{PT} = C_{P0}\left(\frac{4}{3}\pi R^3\right). \tag{10}$$

Considering that the initial particle concentration (C_{P0}) in the simulation was assumed to be 180.3 ppm or 1.2526 mol/m^3; the total particle mass immersed in a spherical tank of 2 m of radius is 6.042 kg.

The percentage of deposited particles at the bottom of the spherical tank ($\%M_{dep}$) can be calculated by:

$$\%M_{dep} = \frac{M_P}{M_{PT}} \times 100\,. \tag{11}$$

Table 2 and Figure 4 show the percentage of deposited particles at the bottom of the spherical tank ($\%M_{dep}$) at different temperatures and particle diameters.

	%*Mdep*				
***dp*, nm**	**340 °C**	**350 °C**	**360 °C**	**370 °C**	**380 °C**
1500	0.476	0.525	0.542	0.582	0.588
1250	0.375	0.402	0.413	0.415	0.425
1000	0.269	0.287	0.305	0.325	0.349
750	0.158	0.175	0.178	0.179	0.192
500	0.070	0.079	0.080	0.084	0.089
400	0.045	0.050	0.051	0.054	0.057
300	0.025	0.028	0.029	0.030	0.032
250	0.018	0.020	0.020	0.021	0.022
200	0.012	0.014	0.014	0.014	0.015
150	0.009	0.009	0.009	0.010	0.010
100	0.007	0.007	0.007	0.007	0.007
50	0.005	0.006	0.006	0.006	0.006
10	0.005	0.005	0.005	0.005	0.005
1	0.005	0.005	0.005	0.005	0.005

Table 2. Percentage of deposited particles at the bottom of the spherical tank ($\%M_{dep}$) containing MoO_3 particles immersed in Athabasca bitumen at different temperatures

Figure 4 demonstrates that the percentage of deposited particles at the bottom of the tank is less than 0.02%, when particle diameters below 200 nm are employed; and, when particle diameters in the range 200 – 1500 nm are used, the percentage of deposited particles is between 0.02 and 0.6 %.

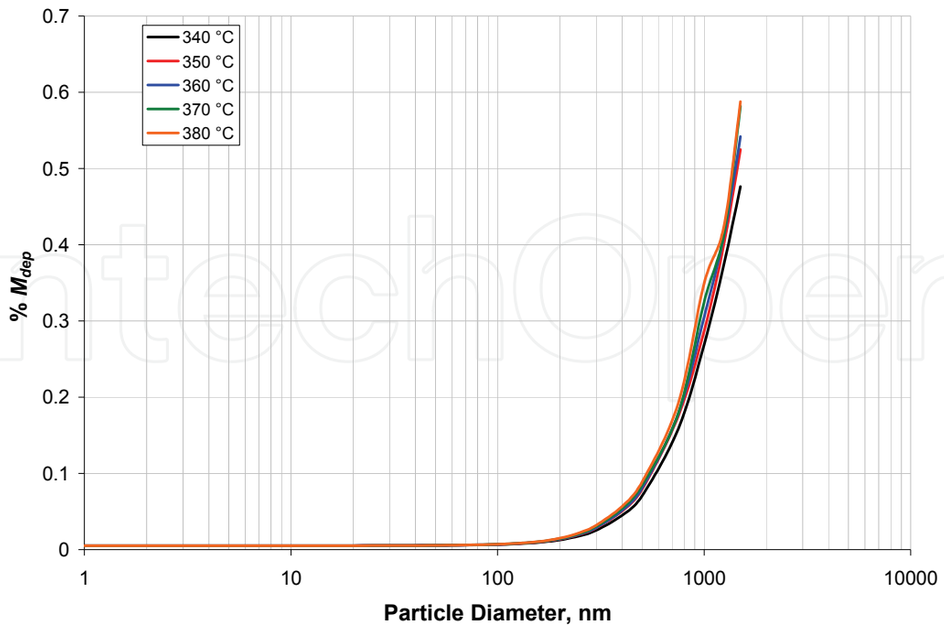

Fig. 4. Percentage of deposited particles at the bottom of the spherical tank (%M_{dep}) at different temperatures and particle diameters for the deposition of MoO_3 particles immersed in Athabasca bitumen enclosed in a spherical tank of 4 m diameter

3. Three-dimensional transport of particles through viscous fluid media

3.1 Three-dimensional convective-dispersive model to predict the concentration profile of particles immersed in viscous media

3.1.1 Axial varticle velocity

The first step to develop the three-dimensional convective-dispersive model is to obtain the flow velocity profile since particle velocity in this direction depends on it. This profile can be obtained from the Navier-Stokes equations. Consider a laminar incompressible fluid that travels inside a horizontal cylinder of radius R and length L. The force (F) pushing the liquid through the cylinder is the change in pressure (ΔP) multiplied by the cross-sectional area of the cylinder (A):

$$F = -\Delta P A \,. \tag{12}$$

This force is oriented in the same direction of the motion of the liquid:

$$\Delta P = P_{out} - P_{in} \,,\; P_{out} < P_{in}. \tag{13}$$

If the cylinder is long enough, then the flow through the cylinder is known as fully developed velocity profile, this means that there are not velocity components in the radial (v_r) and angular direction (v_θ) and the velocity in the longitudinal direction (v_z) is only a function of the radial coordinate (r).

Assuming a fully developed velocity profile at steady state, that the gravity force is not the force causing the motion and its effect is negligible, that the pressure decreases linearly across the length of the cylinder, that the axial velocity (v_z) is finite at r = 0 and that there is a

no slip boundary condition at the cylinder wall; then, the following parabolic velocity profile can be obtained:

$$v_z(r) = \frac{\Delta P}{4\mu_L L} R^2 \left(1 - \frac{r^2}{R^2}\right). \tag{14}$$

Equation 14 is known as the Poiseuille's flow inside cylinders. The volumetric flux (Q) inside the cylinder can be calculated using the following procedure:

$$Q = \int_A \mathbf{n} \cdot \mathbf{v} dA = 2\pi \int_0^R v_z(r) r dr = \frac{\pi \Delta P R^4}{8\mu_L L}. \tag{15}$$

where **n** is the unit vector normal to the velocity vector (**v**). The mean axial velocity ($\overline{v}_z$) is the volumetric flux divided by the cross-sectional area:

$$\overline{v}_z = \frac{2\pi \int_0^R v_z(r) r dr}{\pi R^2} = \frac{\Delta P R^2}{8\mu_L L}. \tag{16}$$

If the particles travelling through a horizontal cylinder are small enough as compared with the size of the cylinder radius, it can be considered that they travel at the same velocity of the fluid. Unlike liquid molecules present in a Poiseulle's flow, a solid spherical discrete particle of radius (r_p) cannot approach the slow flowing area close to the wall (Fung, 1993; Michaelides, 2006). Considering this assumption its average velocity can be calculated by:

$$\overline{v}_z(r_p) = \frac{2\pi \int_0^{R-r_p} v_z(r) r dr}{\pi (R - r_p)^2} = \frac{\Delta P R^2}{8\mu_L L} \left[2 - \left(1 - \frac{r_p}{R}\right)^2\right]. \tag{17}$$

If r_p << R, then

$$\overline{v}_z(r_p) = \frac{\Delta P R^2}{8\mu_L L} = \overline{v}_z. \tag{18}$$

Thus, the axial velocity of the particles can be represented by the Poiseuille's flow equation.

3.1.2 Analysis of the particle concentration inside a horizontal cylindrical channel

Particle concentration in a fluid medium can be obtained by carrying out a mass balance for particles present in a differential element of the system. In order to develop a convective-dispersive model which simulates the transport of particles travelling through a fluid medium, the mass balance for particles present in a differential element of a cylinder presented in Section 2.1 can be employed. Consider a laminar incompressible flow which contains particles that flow inside a horizontal cylinder of radius R and length L. The mass balance equation that represents this problem is the following (Bird et al., 2007):

$$\frac{\partial C_P}{\partial t} + \left(v_r \frac{\partial C_P}{\partial r} + v_\theta \frac{1}{r} \frac{\partial C_P}{\partial \theta} + v_z \frac{\partial C_P}{\partial z}\right) = D_E \left[\frac{1}{r} \frac{\partial}{\partial r}\left(r \frac{\partial C_P}{\partial r}\right) + \frac{1}{r^2} \frac{\partial^2 C_P}{\partial \theta^2} + \frac{\partial^2 C_P}{\partial z^2}\right]. \tag{19}$$

The settling of particles affects the distribution of the particle concentration at each point of the horizontal cylinder. Thus, the particle concentration inside the horizontal channel will be modelled as a function of the position of the particles inside the channel and the time: $C_P = C_P(r, \theta, z, t)$.

Equation 19 can be simplified by assuming that the angular velocity of the particle (v_θ) is small compared to the radial velocity (v_r). Thus, v_θ can be neglected. Equation 19 can be written as:

$$\frac{\partial C_P}{\partial t} + \left(v_r \frac{\partial C_P}{\partial r} + v_z \frac{\partial C_P}{\partial z} \right) = D_E \left[\frac{1}{r} \frac{\partial}{\partial r} \left(r \frac{\partial C_P}{\partial r} \right) + \frac{1}{r^2} \frac{\partial^2 C_P}{\partial \theta^2} + \frac{\partial^2 C_P}{\partial z^2} \right]. \tag{20}$$

As in Section 2.1, the radial particle velocity (v_r) is considered to be the projection of the vertical terminal velocity of the particle (v_{pT}) into the radial direction:

$$v_r = v_{pT} \cos\theta = \frac{g\left(\rho_p - \rho_L\right) d_p^2}{18 \mu_L} \cos\theta. \tag{21}$$

In the case of the axial velocity (v_z), it has been shown that it can be represented by the Poiseuille's flow. Equation 20 can now be expressed as:

$$\frac{\partial C_P}{\partial t} + \left[v_{pT} \cos\theta \frac{\partial C_P}{\partial r} + \frac{\Delta P}{4 \mu_L L} R^2 \left(1 - \frac{r^2}{R^2} \right) \frac{\partial C_P}{\partial z} \right] = D_E \left[\frac{1}{r} \frac{\partial}{\partial r} \left(r \frac{\partial C_P}{\partial r} \right) + \frac{1}{r^2} \frac{\partial^2 C_P}{\partial \theta^2} + \frac{\partial^2 C_P}{\partial z^2} \right]. \tag{22}$$

Initially ($t = 0$), it is assumed that the cylinder only contains the fluid travelling through it and there are no particles present inside the cylindrical channel.

$$\text{At } t = 0, \; C_P(r, \theta, z, 0) = 0, \quad 0 \le r \le R, \; 0 \le \theta \le 2\pi, \; 0 \le z \le L. \tag{23}$$

If an open system is considered, at the entrance of the channel ($z = 0$) the suspension of solid particles has a homogeneous constant initial concentration (C_{P0}).

$$\text{At } z = 0, \quad C_P(r, \theta, 0, t) = C_{P0}, \quad 0 \le r \le R, \; 0 \le \theta \le 2\pi. \tag{24}$$

At the exit of the channel ($z = L$) the convection dominates the mass transport; this implies that the concentration gradient due to dispersion in a perpendicular direction to this boundary is negligible. This condition eliminates the need of specifying a concentration or a fixed value for the flux at the outlet boundary, since both of them are unknown. Mathematically this condition can be represented by:

$$\mathrm{n} \cdot \left(-D_E \nabla C_P \right) = 0 \Rightarrow \mathrm{e}_z \cdot \left[-D_E \left(\mathrm{e}_r \frac{\partial C_P}{\partial r} + \frac{\mathrm{e}_\theta}{r} \frac{\partial C_P}{\partial \theta} + \mathrm{e}_z \frac{\partial C_P}{\partial z} \right) \right] = 0 \,, \tag{25}$$

where **n** is the normal vector to the plane at the outlet of the cylinder, $\mathbf{e}_z$, in this case. Solving the dot product, it is found that:

$$\text{At } z = L, \; \frac{\partial C_P}{\partial z} = 0, \quad 0 \le r \le R, 0 \le \theta \le 2\pi. \tag{26}$$

In the vertical axis there are symmetry boundary conditions that can be mathematically represented as:

$$-D_E\left(\frac{1}{r}\frac{\partial C_P}{\partial \theta}\right)+v_\theta C_P=0. \tag{27}$$

Previously it was assumed that the angular velocity of the particle (v_θ) is neglected, therefore:

$$\text{At } \theta=0,\ \frac{\partial C_P}{\partial \theta}=0\ ,\quad 0\le r\le R,\ 0\le\ z\le L. \tag{28}$$

$$\text{At } \theta=\pi,\ \frac{\partial C_P}{\partial \theta}=0\ ,\quad 0\le r\le R,\ 0\le z\ \le L. \tag{29}$$

The particle concentration is finite along the radial direction for all the angles and lengths:

$$\text{At } 0\le\ r\ \le R,\ C_P=\textit{finite}\ ,\quad 0\le\theta\le 2\pi,\ 0\le z\le L. \tag{30}$$

The walls of the channel represent a physical boundary where there is no mass exchange between the interior and exterior of the cylinder. This is an insulation boundary that will prevent any particle from leaving the channel and gather all them at the bottom. The insulation boundary means that there is no convective or dispersive flux across that boundary. This can be represented by:

$$-D_E\left(\frac{\partial C_P}{\partial r}\right)+v_r C_P=0\ . \tag{31}$$

Then:

$$\text{At } r=R,\ -D_E\frac{\partial C_P}{\partial r}+\left(v_{pT}\cos\theta\right)C_P=0\ ,\quad 0\le\theta\le 2\pi,\ 0\le z\le L. \tag{32}$$

The convective-dispersive model is a linear second order parabolic partial differential equation. A numerical solution based in the finite element method was used in this work. Computational fluid dynamics software was used to apply the method.

3.2 Effect of the fluid medium properties on the dispersion coefficient

This section is dedicated to study the variation of the dispersion coefficient (D_E) respect to changes in the properties of the fluid medium and the initial concentration of particles. For this study, experimental data collected from a previous work (Loria et al., 2010) was employed.

Figure 5 shows the behaviour of the dispersion coefficient with respect to an increase of density and viscosity of the fluid medium. It can be observed that as the fluid medium becomes denser and more viscous the dispersion coefficient decreases because particles lose their ability to move from high concentrated areas to low concentrated ones.

Figure 6 shows the variation of the dispersion coefficient with respect to a change of the fluid velocity. It can be observed that as fluid velocity increases the dispersion coefficient decreases. In this case an increase in the fluid velocity causes an increase in the axial velocity of the particles, enhancing their ability to remain suspended and reducing their capacity to move from high concentrated areas to low concentrated ones, causing a decrease in the dispersion coefficient.

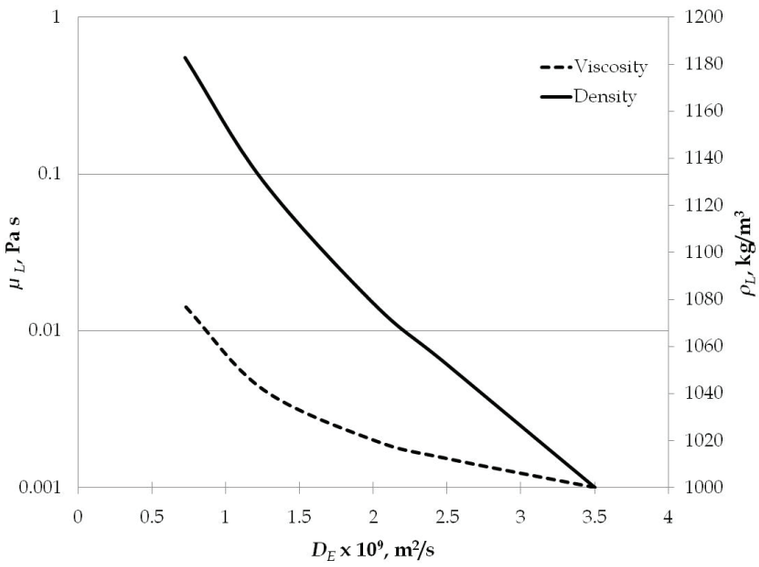

Fig. 5. Dispersion coefficient (D_E) as a function of the viscosity (μ_L) and density (ρ_L) of the fluid medium in a horizontal cylinder

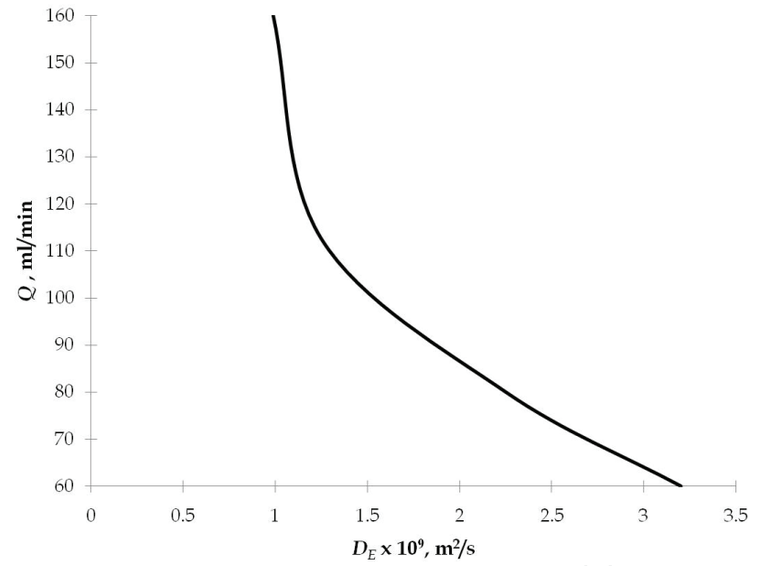

Fig. 6. Dispersion coefficient (D_E) as a function of the fluid velocity (Q) of the fluid medium in a horizontal cylinder

Several works regarding axial dispersion coefficients in horizontal channels were found in the reviewed literature. Nevertheless, large part of this literature is advocated to aerosol particles flowing through airways. For instance, Zhang et al. (2005) and Schulz et al. (2000) have studied the aerosol particle dispersion coefficients to determine how many and where these particles are deposited in the human respiratory system. Giojelli et al. (2001) have focused their attention to study the dispersion coefficients for aerosol particles separation from biogas produced by sludge coming from wastewaters. The typical orders of magnitude

for dispersion coefficients employed in the previously described processes were around 10^{-4} m^2/s, which is not by any means comparable to the ones obtained in the previously referred work (Loria et al., 2010), since totally different materials are involved in the mass transfer of the studied phenomena.

The dispersion of a solute in a laminar Poiseuille's flow to measure diffusion coefficients of proteins and macro-molecules was studied by Bello et al.(1994). Their experimental measurements of the diffusion coefficients gave values that varied from 10^{-8} to 10^{-11} m^2/s. Even though these results are closer to the dispersion coefficients calculated the work from Loria et al. (2010), they cannot serve as a standard of comparison, since the diameter of these molecules is reduced to a few nanometers and the vessels where these authors evaluated the diffusion coefficients were capillaries with 50 to 100 μm of inner diameter.

3.3 Ultradispersed catalytic particles immersed in bitumen at upgrading temperatures transported through a pipeline

This section is dedicated to the application of the three-dimensional convective-dispersive model to a large scale case which involves the transport of MoO_3 catalytic particles immersed in Athabasca bitumen, at upgrading conditions (340-380 °C), through a pipe of 100 m length and 101.6 cm diameter.

The simulations in this section have two different goals. The first is to find the critical diameter to avoid particle deposition. The second is to calculate the deposited particle mass at the bottom of the pipe once the steady state has been reached.

As in the previous section, the density (ρ_L) and viscosity (μ_L) of the Athabasca bitumen at five different temperatures ranging from 340 to 380 °C were employed in the simulations for this section. These physical properties of the Athabasca bitumen at the temperatures of interest were shown in Table 1.

In this section, twelve different MoO_3 particle diameters were used for the simulations: 1, 10, 50, 100, 150, 200, 250, 300, 400, 500, 1000 and 1500 nm. The initial MoO_3 particle concentration (C_{P0}) that was applied to all the simulations was 1.2526 mol/m^3, equivalent to 180.3 ppm.

A fluid velocity (Q) of 30000 ml/min (5×10^{-4} m^3/s or 272 bbd) was chosen in order to have a large volumetric flux and, also, to maintain a laminar regime inside the pipe. Taking into account that the pipe diameter is d = 101.6 cm, the mean axial velocity ($\overline{v}_z = Q/(\pi\, d^2/4)$) is 6.17×10^{-4} m/s. This value permits the calculation of the fluid Reynolds number ($Re = \rho_L\, \overline{v}_z\, d/\mu_L$) which estimates if a fluid is laminar or turbulent.

Table 3 shows the different values of the fluid Reynolds number for the Athabasca bitumen transported through a pipe at the 5 different studied temperatures. Also, Table 3 shows the pressure drop (ΔP) between the ends of the pipe which was calculated using Equation 18.

T, °C	ρ_L, kg/m³	μ_L, cP	ΔP, mPa	Re
340	884.7	2.71	5.18	204
350	877.2	2.42	4.63	227
360	869.4	2.38	4.55	229
370	856.4	2.27	4.34	236
380	843.7	2.17	4.15	244

Table 3. Fluid Reynolds numbers and pressure drop between the ends of the pipe at the 5 different studied temperatures

Table 3 reports fluid Reynolds numbers <2100 and small values of pressure drop between the ends of the cylinder which demonstrates that a laminar flow is maintained across the pipe at any of the 5 different studied temperatures. Generally, a fluid is laminar if the Reynolds number is between 0 and 2100 (Bird et al., 2007).

The calculation of the dispersion coefficient that was employed for these simulations was based on the results that were obtained when the three-dimensional convective-dispersive model was validated with Fe_2O_3 particles immersed in mixtures of water and glycerol (Loria et al., 2010). These results were taken into account because particle properties and concentration as well as the fluid medium characteristics and axial velocities used in that experiments are similar to those present in the simulations carried out in this section.

The dispersion coefficient calculation was carried out in a similar way as in Section 2.3: polynomial interpolations were carried out with the data from Figure 5 and Figure 6 (μ_L and ρ_L vs. D_E and $\overline{v}_z$ vs. D_E); then, for each temperature three different values of D_E were obtained (based on μ_L, C_{P0} and in $\overline{v}_z$) and their average was recorded; finally, the 5 different D_E average values (corresponding to each studied temperature and ranging from 2.1 - 2.18 × 10^{-9} m^2/s) were averaged and the final D_E value was obtained. The D_E value obtained from these calculations resulted to be 2.14 × 10^{-9} m^2/s.

A total of 60 different simulations were carried out in this section (based on the 12 different particle diameters and 5 different temperatures). Computational fluid dynamics was used to perform the simulations; each simulation was carried out up to a time of 1.5 × 10^7 s (4167 h), a time long enough to reach the steady state in each one of them. 9878 grid points were employed for the solution of each simulation and their computing time was around 240 s.

One subject of interest in this study is the critical particle diameter for deposition. In order to measure this parameter, the following analysis was conducted.

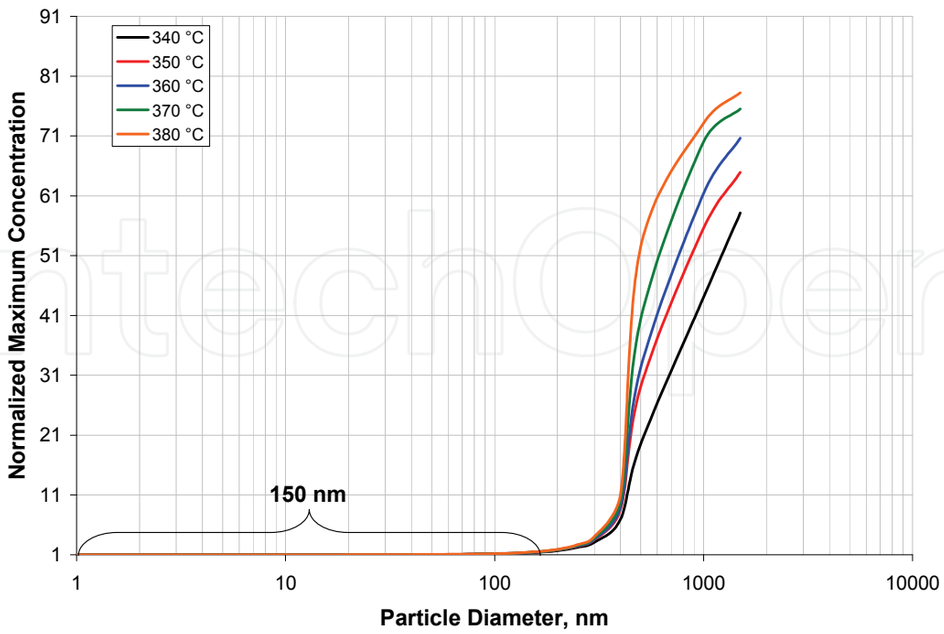

Fig. 7. Effect of the particle diameter and temperature on the deposition of MoO_3 particles immersed in Athabasca bitumen flowing through a pipe

The normalized maximum particle concentration, which in this case is the concentration that is found at the exit bottom of the horizontal cylinder after the simulation time (steady state) divided by the initial concentration, was calculated for each simulation. This normalized maximum particle concentration was plotted against the particle diameter in order to observe at which particle diameter the maximum particle concentration becomes significant. Figure 7 represents the behaviour of the normalized maximum particle concentration at different particle diameters and temperatures.

As temperature increases for a specific particle diameter, the normalized maximum concentration increases and as the particle diameter increases, the normalized maximum concentration increases for a specific temperature. It can also be observed that a change in particle diameter have a more pronounced effect over the normalized maximum concentration than a change in temperature.

In the particle diameter axis, there is a zone for values lower than 150 nm where the normalized maximum concentration is equal to the initial independently of the temperature. This means that MoO_3 particles smaller than 150 nm will remain flowing through the Athabasca bitumen after a long period of time (1.5×10^7 s) in the range of temperatures from 340 to 380 °C.

The following procedure was employed for the calculation of the deposited mass of the catalytic particles along the bottom of the pipe once the steady state has been reached.

Assuming that the deposited particles filled a small horizontal section of height H at the bottom of a cylinder of radius R and length L, its volume (V_P) can be calculated by:

$$V_P = L\left[\cos^{-1}\left(\frac{R-H}{R}\right)R^2 - \sqrt{H(2R-H)}(R-H)\right]. \tag{33}$$

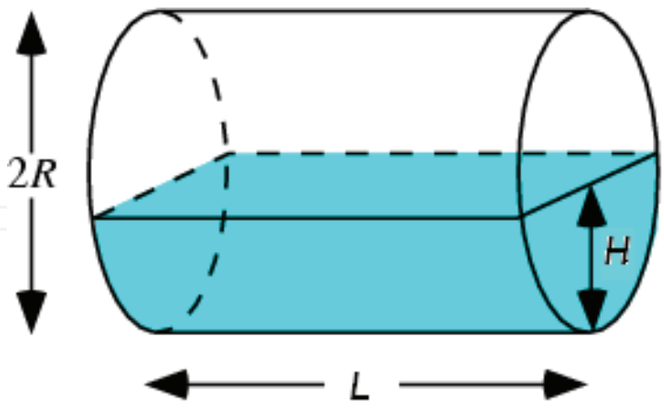

Fig. 8. Horizontal section of height H at the bottom of a cylinder of radius R and length L

Assuming that the height of this small gap is approximately H = 3.5 cm (based on graphics from the simulations), the volume of the small horizontal section (V_P) for a cylinder of 101.6 cm of radius and 100 m of length is 0.871 m^3.

The average particle concentration ($\overline{C}_{P\max}$) at the bottom of the channel and across the length L of the cylinder after a long period of time ($t = 1.5 \times 10^7$ s) can be estimated by:

$$\bar{C}_{P\max} = \frac{\int_0^L C_P(L)\,dL}{L}. \tag{34}$$

The different concentrations along the bottom of the cylinder can be retrieved from the simulation results; with these data the integral in Equation 34 can be evaluated using the Simpson's rule for the solution of numerical integrals (Carnahan et al., 1969).
The mass of particles deposited at the bottom of the channel (M_P), enclosed in the partial volume (V_P) with height H, is:

$$M_P = \bar{C}_{P\max} V_P\,. \tag{35}$$

On the other hand, the total mass of particles that entered to the tank (M_{PT}) after a long period of time ($t = 1.5 \times 10^7$ s) can be estimated by:

$$M_{PT} = QC_{P0}t\,. \tag{36}$$

Considering that the initial particle concentration (C_{P0}) in the simulation was assumed to be 180.3 ppm or 1.2526 mol/m^3 and that the volumetric flux is $Q = 5 \times 10^{-4}$ m^3/s, the total particle mass that entered to the cylinder after 1.5×10^7 s was 1352 kg. The percentage of deposited particles at the bottom of the spherical tank (%M_{dep}) can be calculated by Equation 11.

	%M_{dep}				
d_p, nm	**340 °C**	**350 °C**	**360 °C**	**370 °C**	**380 °C**
1500	0.488	0.565	0.615	0.657	0.681
1000	0.372	0.484	0.534	0.610	0.637
500	0.142	0.203	0.218	0.264	0.327
400	0.056	0.067	0.070	0.076	0.084
300	0.029	0.031	0.032	0.034	0.035
250	0.022	0.023	0.024	0.024	0.025
200	0.017	0.018	0.018	0.019	0.019
150	0.015	0.015	0.015	0.015	0.015
100	0.013	0.013	0.013	0.013	0.013
50	0.012	0.012	0.012	0.012	0.012
10	0.012	0.012	0.012	0.012	0.012
1	0.012	0.012	0.012	0.012	0.012

Table 4. Percentage of deposited particles at the bottom of the horizontal cylinder (%M_{dep}) containing MoO_3 particles immersed in Athabasca bitumen at different temperatures

The percentage of deposited particles at the bottom of the spherical tank (%M_{dep}) at different temperatures and particle diameters is shown in Table 4 and Figure 9.
In Figure 9, it can be observed that after the studied time, less than 0.1 % of the total mass of particles, with diameters lower than 400 nm, has been deposited; whereas the percentage of deposited particles, with diameters in the range 400 – 1500 nm, is between 0.1 and 0.68 %.

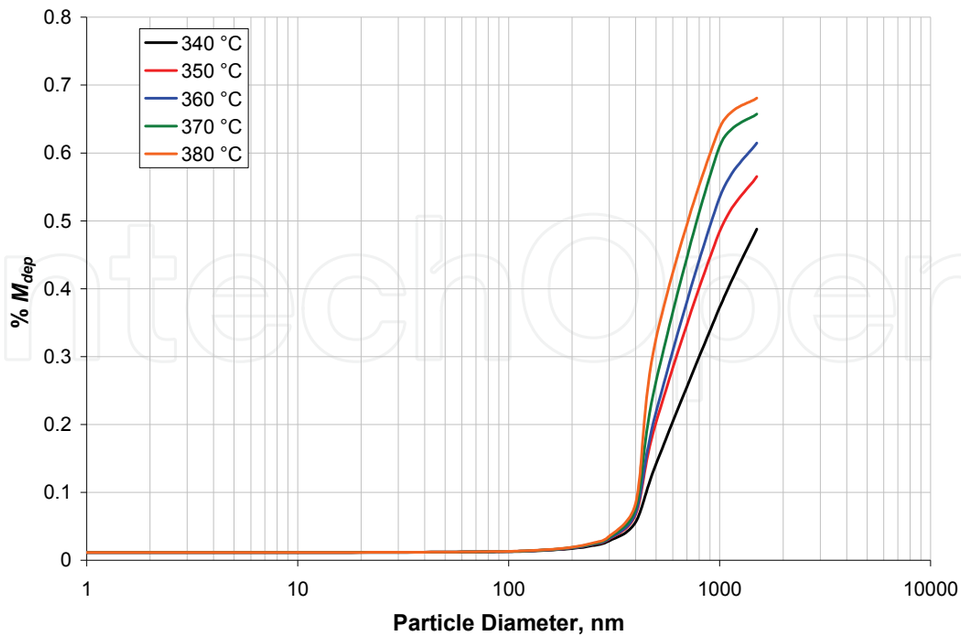

Fig. 9. Percentage of deposited particles at the bottom of the cylindrical channel (%M_{dep}) at different temperatures and particle diameters for the deposition of MoO_3 particles immersed in Athabasca bitumen flowing through a pipe

4. Conclusion

The results from these simulations unveiled the particle diameter and fluid medium properties that are necessary to ensure particle suspension and mobility in bitumen. In the case of the spherical storage tank simulation, it was found that MoO_3 particles smaller than 150 nm will remain suspended in bitumen at temperatures from 340 to 380 °C after a long period of time (27778 h) Also, it was shown that the percentage of deposited particles at the bottom of the tank after this period of time is less than 0.02 % when particles diameters below 200 nm are utilized.

Regarding the simulations applied to the flow of particles through a horizontal pipeline, the results demonstrated that particles smaller than 150 nm will remain flowing through bitumen after a long period of time (4167 h) in the range of temperatures from 340 to 380 °C. In addition, the modelling results showed the percentage of settled particles at the bottom of the cylinder after this period of time when a particle deposition scenario is presented. It was observed that less than 0.1 % of the total mass of particles (that passed through the cylinder during this time), with diameters lower than 400 nm, were deposited at the bottom.

Based on these results, it seems that when MoO_3 catalytic particles with diameters lower than 400 nm (nanometric range) are immersed in bitumen either in a stagnant or a flow scenario, almost all the particles will remain suspended in the system. Therefore, this kind of particles could be employed as ultradispersed catalysts for bitumen hydroprocessing reactions. It would be interesting to compare these models with experimental data from real systems; however, on line tools for the particle concentration measurement would have to be developed in order to achieve this objective.

5. Acknowledgment

This work was supported in part by the National Council for Science and Technology of Mexico, The Alberta Ingenuity Centre for In Situ Energy funded by the Alberta Ingenuity Fund and the industrial sponsors: Shell International, ConocoPhillips, Nexen Inc, Total Canada and Repsol-YPF, and The Schulich School of Engineering at the University of Calgary, Canada.

6. References

Adamczyk, Z. & Van De Ven, T. G. M. (1981). Deposition of Particles under External Forces in Laminar Flow through Parallel-plate and Cylindrical Channels. Journal of Colloid and Interface Science, Vol. 80 No. 2 pp. 340-356

Bello, M. S., Rezzonico, R. & Righetti, P. G. (1994). Use of Taylor-Aris Dispersion for Measurement of a Solute Diffusion Coefficient in Thin Capillaries. Science, Vol. 266 No. 5186 pp. 773-776

Bird, R. B., Stewart, W. E. & Lightfoot, E. N. (2007). Transport Phenomena, J. Wiley, New York

Carnahan, B., Luther, H. A. & Wilkes, J. O. (1969). Applied Numerical Methods, Wiley, New York

d'Orlyé, F., Varenne, A. & Gareil, P. (2008). Determination of Nanoparticle Diffusion Coefficients by Taylor Dispersion Analysis using a Capillary Electrophoresis Instrument. Journal of Chromatography A, Vol. 1204 No. 2 pp. 226-232

Franco, A. (May, 2008). Transport Phenomena, Available from http://www.sc.ehu.es/sbweb/fisica/transporte

Fung, Y. C. (1993). Biomechanics: Mechanical Properties of Living Tissues, Springer, New York

Galarraga, C. E. & Pereira-Almao, P. (2010). Hydrocracking of Athabasca Bitumen Using Submicronic Multimetallic Catalysts at Near In-Reservoir Conditions. Energy & Fuels, Vol. 24 No. 4 pp. 2383-2389

Giojelli, B., Verdier, C., Hihn, J. Y., Béteau, J. F. & Rozzi, A. (2001). Identification of Axial Dispersion Coefficients by Model Method in Gas/Liquid/Solid Fluidised Beds. Chemical Engineering and Processing, Vol. 40 No. 2 pp. 159-166

Loria, H., Pereira-Almao, P. & Satyro, M. (2009a). Prediction of Density and Viscosity of Bitumen Using the Peng-Robinson Equation of State. Industrial & Engineering Chemistry Research, Vol. 48 No. 22 pp. 10129-10135

Loria, H., Pereira-Almao, P. & Scott, C. E. (2009b). A Model To Predict the Concentration of Dispersed Solid Particles in an Aqueous Medium Confined inside Horizontal Cylindrical Channels. Industrial & Engineering Chemistry Research, Vol. 48 No. 8 pp. 4088-4093

Loria, H., Pereira-Almao, P. & Scott, C. E. (2009c). A Model To Predict the Concentration of Submicrometer Solid Particles in Viscous Media Confined inside Horizontal Cylindrical Channels. Industrial & Engineering Chemistry Research, Vol. 48 No. 8 pp. 4094-4100

Loria, H., Pereira-Almao, P. & Scott, C. E. (2010). Model To Predict the Concentration of Ultradispersed Particles Immersed in Viscous Media Flowing through Horizontal Cylindrical Channels. Industrial & Engineering Chemistry Research, Vol. 49 No. 4 pp. 1920-1930

Loria, H., Trujillo-Ferrer, G., Sosa-Stull, C. & Pereira-Almao, P. R. (2011). Kinetic Modeling of Bitumen Hydroprocessing at In-Reservoir Conditions employing Ultradispersed Catalysts. Energy & Fuels, *In Press*

Massabò, M., Catania, F. & Paladino, O. (2007). A New Method for Laboratory Estimation of the Transverse Dispersion Coefficient. Ground Water, Vol. 45 No. 3 pp. 339-347

Michaelides, E. E. (2006). Particles, Bubbles & Drops: Their Motion, Heat and Mass Transfer, World Scientific, New Jersey

Pereira-Almao, P. (2007). Fine Tuning Conventional Hydrocarbon Characterization to Highlight Catalytic Upgrading Pathways, Proceedings of Variability of the Oil Sands Resource Workshop, Lake Louise, AB, May 1-4, 2007

Pereira-Almao, P., Hill, J., Wang, J. & Vasquez, A. (2005). Ultra Dispersed Catalyst for Processing Heavy Hydrocarbon Fractions, Proceedings of AICHE, 2005 Spring National Meeting, Atlanta, GA, USA

Pereira-Almao, P. R., Ali-Marcano, V., Lopez-Linares, F. & Vasquez, A. (2007).Ultradispersed Catalysts Compositions and Methods of Preparation. WO 2007/059621 A1, 2007.

Perry, R. H. (1997). Perry's Chemical Engineers' Handbook, McGraw-Hill, New York

Ramalho, R. S. (1983). Introduction to Wastewater Treatment Processes, Academic Press, New York

Robbins, G. A. (1989). Methods for Determining Transverse Dispersion Coefficients of Porous Media in Laboratory Column Experiments. Water Resources Research, Vol. 25 No. 6 pp. 1249-1258

Schulz, H., Brand, P. & Heyder, J. (2000). Particle Deposition in the Respiratory Tract, In: Particle-Lung Interactions, P. Gehr and J. Heyder, (Ed.), 229-290, Marcel Dekker, New York

Zhang, Z., Kleinstreuer, C., Donohue, J. F. & Kim, C. S. (2005). Comparison of Micro- and Nano-size Particle Depositions in a Human Upper Airway Model. Journal of Aerosol Science, Vol. 36 No. 2 pp. 211-233

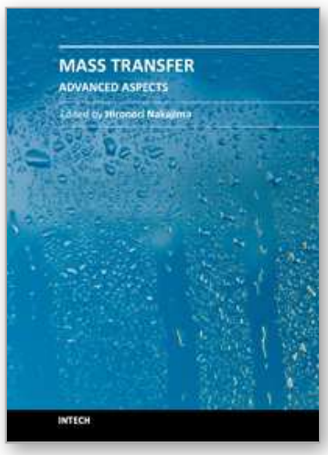

Mass Transfer - Advanced Aspects

Edited by Dr. Hironori Nakajima

ISBN 978-953-307-636-2
Hard cover, 824 pages
Publisher InTech
Published online 07, July, 2011
Published in print edition July, 2011

Our knowledge of mass transfer processes has been extended and applied to various fields of science and engineering including industrial and manufacturing processes in recent years. Since mass transfer is a primordial phenomenon, it plays a key role in the scientific researches and fields of mechanical, energy, environmental, materials, bio, and chemical engineering. In this book, energetic authors provide present advances in scientific findings and technologies, and develop new theoretical models concerning mass transfer. This book brings valuable references for researchers and engineers working in the variety of mass transfer sciences and related fields. Since the constitutive topics cover the advances in broad research areas, the topics will be mutually stimulus and informative to the researchers and engineers in different areas.

INTECH
open science | open minds

InTech Europe
University Campus STeP Ri
Slavka Krautzeka 83/A
51000 Rijeka, Croatia
Phone: +385 (51) 770 447
Fax: +385 (51) 686 166
www.intechopen.com

InTech China
Unit 405, Office Block, Hotel Equatorial Shanghai
No.65, Yan An Road (West), Shanghai, 200040, China
中国上海市延安西路65号上海国际贵都大饭店办公楼405单元
Phone: +86-21-62489820
Fax: +86-21-62489821

IntechOpen